doi:10.1093/plphys/kiab180 PLANT PHYSIOLOGY 2021: 186: 1734–1746

Plant Physiology®

Research Report

CYTOKININ-RESPONSIVE GROWTH REGULATOR regulates cell expansion and cytokinin-mediated cell cycle progression

Joonghyuk Park,[1] Seungchul Lee ,[1] Geuntae Park,[2] Hyunwoo Cho,[1,†] Daeseok Choi ,[3] Masaaki Umeda ,[4] Yeonhee Choi ,[2] Daehee Hwang[2] and Ildoo Hwang [1,*,‡]

1 Department of Life Sciences, Pohang University of Science and Technology, Pohang 37673, Korea
2 School of Biological Sciences, Seoul National University, Seoul 151-747, Korea
3 School of Interdisciplinary Bioscience and Bioengineering, Pohang University of Science and Technology, Pohang 37673, Korea
4 Graduate School of Science and Technology, Nara Institute of Science and Technology, Takayama 8916-5, Ikoma, Nara 630-0192, Japan

*Author for communication: ihwang@postech.ac.kr
†Present address: Department of Industrial Plant Science & Technology, Chungbuk National University, Cheongju 28644, Korea.
‡Senior author.

These authors contributed equally to this work (J.P., S.L.).

J.P., S.L, and I.H. designed this study. S.L., D.C., and D.H. analyzed and processed the microarray data. J.P. and S.L. performed transgenic, cell biological, and other functional analyses. G.P. performed phenotypic analysis of embryos and floral organs. M.U. performed ploidy analysis. H.C. performed the EdU staining assay. J.P., S.L., and I.H. wrote the manuscript. Y.C., M.U., and I.H. supervised the work.

The author responsible for distribution of materials integral to the findings presented in this article in accordance with the policy described in the Instructions for Authors (https://academic.oup.com/plphys/pages/general-instructions) is: Ildoo Hwang (ihwang@postech.ac.kr).

Abstract

The cytokinin (CK) phytohormones have long been known to activate cell proliferation in plants. However, how CKs regulate cell division and cell expansion remains unclear. Here, we reveal that a basic helix–loop–helix transcription factor, CYTOKININ-RESPONSIVE GROWTH REGULATOR (CKG), mediates CK-dependent regulation of cell expansion and cell cycle progression in *Arabidopsis thaliana*. The overexpression of *CKG* increased cell size in a ploidy-independent manner and promoted entry into the S phase of the cell cycle, especially at the seedling stage. Furthermore, CKG enhanced organ growth in a pleiotropic fashion, from embryogenesis to reproductive stages, particularly of cotyledons. In contrast, *ckg* loss-of-function mutants exhibited smaller cotyledons. CKG mainly regulates the expression of genes involved in the regulation of the cell cycle including *WEE1*. We propose that *CKG* provides a regulatory module that connects cell cycle progression and organ growth to CK responses.

Introduction

Cytokinins (CKs) are a class of phytohormones that regulate numerous growth and development processes such as cell proliferation and fate determination, vasculature development, sink/source relationship, leaf senescence, stress, and defense responses, as well as responses to environmental cues (Roitsch and Ehneß, 2000; Mähönen et al., 2006; Hejatko et al., 2009; Choi et al., 2010; Nishiyama et al., 2011; Raines et al., 2016; Arnaud et al., 2017; Poitout et al., 2018; reviewed in Hwang et al., 2012; Kieber and Schaller, 2018; Cortleven et al., 2019; Wybouw and De Rybel, 2019).

CKs are perceived by a series of two-component histidine kinase receptors located at the plasma membrane or the

Received October 21, 2020. Accepted March 31, 2021. Advance access publication April 28, 2021

endoplasmic reticulum (ER): ARABIDOPSIS HISTIDINE KINASE (AHK) AHK2, AHK3, and AHK4, also known as CYTOKININ RESPONSE1 (CRE1) and WOODENLEG (WOL). Activated receptors then phosphorylate ARABIDOPSIS PHOSPHOTRANSFER PROTEINs, which act as shuttles between the plasma membrane or the ER and the nucleus to phosphorylate type-B ARABIDOPSIS RESPONSE REGULATORs (ARRs; reviewed in Hwang et al., 2012; Kieber and Schaller, 2014). Type-B ARRs target various CK-responsive genes, including the negative CK signaling regulators type-A ARRs in a feedback loop (Hwang and Sheen, 2001; Zubo et al., 2017). In addition, CYTOKININ RESPONSE FACTORs, which belong to the ETHYLENE RESPONSE FACTOR/APETALA2 (AP2)-type transcription factors, are involved in CK signaling (Rashotte et al., 2006; Kim, 2016).

CKs also play a critical role in the regulation of stem cell niches in primary meristems. For example, the shoot apical meristem (SAM) of the *ahk2 ahk3 ahk4* triple mutant is much smaller than that of the wild-type (Higuchi et al., 2004; Nishimura et al., 2004). Conversely, the overexpression of a constitutively active form of the type-A ARR7 severely affects SAM formation and subsequent shoot proliferation (Leibfried et al., 2005; Bartrina et al., 2011). Likewise, loss of the CYTOKININ OXIDASE-DEHYDROGENASE (CKX) CK-degrading enzymes increases SAM size in *Arabidopsis thaliana* (Bartrina et al., 2011), whereas a mutation of the CK biosynthetic gene *LONELY GUY4* (*LOG4*) reduces SAM size and perturbs meristem functions in rice (*Oryza sativa*; Kurakawa et al., 2007).

In contrast to the positive role of CKs in SAM cell proliferation, the size of the root apical meristem (RAM) increases in the *ipt3 ipt5 ipt7* triple mutant for the CK biosynthesis genes *ISOPENTENYL TRANSFERASEs* (*IPTs*), as well as in the *ahk3* single mutant and a double mutant of type-B *ARR1* and *ARR12*, due to a reduced differentiation rate of meristematic cells (Dello Ioio et al., 2007). In addition, CKs promote the transition from cell division to cell expansion in the RAM by initiating an early onset of endoreduplication via ARR2 (Takahashi et al., 2013). CKs also induce the expression of the cell cycle regulator *CYCLIN D3* (*CYCD3*), which controls the transition from the G1 to the S phase of the cell cycle in the SAM. In addition, the CK biosynthesis inhibitor lovastatin blocks the G2/M phase transition in tobacco (*Nicotiana tabacum*) cell cultures (Redig et al., 1996; Riou-Khamlichi et al., 1999; Dewitte et al., 2007). It is clear that CK-mediated plant growth and development is tightly associated with the cell-cycle progression machinery, but how they are connected is not fully understood. The opposite mode of action exhibited by CKs between the SAM and RAM suggests that CKs regulate the cell cycle in a cell-type specific manner through different downstream targets or via additional but yet-unknown specific modulators of CK signaling.

In this study, we reveal that CYTOKININ-RESPONSIVE GROWTH REGULATOR (CKG), previously named basic helix–loop–helix (bHLH) transcription factor bHLH137 (Toledo-Ortiz et al., 2003), directly targets cell-cycle regulators and mediates organ growth in a CK-dependent manner in Arabidopsis. We propose that the CK–CKG module provides an important regulatory node for the cell cycle during plant development.

Results

CKG is a novel regulator of CK responses

To identify novel transcription factors that specifically respond to CKs, we first analyzed transcriptome data from a time-course data set that tested the response of Arabidopsis seedlings to the phytohormones abscisic acid, auxin, brassinosteroids, CKs, ethylene, gibberellins, jasmonic acid, and salicylic acid (GSE39384, E-TABM-51), using the systematic analytical tool iNID (Choi et al., 2014). Using non-negative matrix factorization clustering, we classified phytohormone responses into 30 differential expression patterns (DEPs) that described either phytohormone-specific regulation or complex regulation of multiple phytohormones on gene expression (Figure 1A). Among them, three DEPs (arrows in Figure 1A) were associated with CK-specific regulation and designated as clusters C1, C2, and C3 (Figure 1B), containing 457, 237, and 205 genes, respectively. Arabidopsis seedlings were treated with CK for 30 min, 1 h, and 3 h in the original data set, and we observed that each cluster followed a distinct CK response profile. The C1 cluster included genes that were upregulated in response to CKs only at the 3-h time point. In contrast, the C3 cluster consisted of genes induced as early as 30 min after CK treatment and remained highly expressed thereafter. Genes that belonged to the C2 cluster exhibited the opposite expression pattern from those in C3.

To determine whether these three clusters were associated with biological processes related to CKs, we investigated potential enrichment in gene ontology (GO) biological processes represented by their constituent genes (Figure 1C; $P < 0.05$, Supplemental Figure S1). The C3 cluster included genes involved in "cytokinin metabolic process" and "cytokinin-mediated signaling". The C1 cluster was associated with "ribosome biogenesis" and "root development", while genes from the C2 cluster returned the GO biological processes "gibberellin-mediated signaling", "leaf senescence", and "ethylene-mediated signaling pathway". These results suggest that the C3 cluster is tightly connected to CKs, while the other two clusters are not directly linked to CK-mediated responses.

Therefore, we further characterized the genes belonging to cluster C3 to identify new regulators of CK responses: we selected a set of transcription factor-encoding genes that (1) were co-expressed with primary CK-responsive *ARRs* (*ARR3/4/5/6/7/8/15/16*) and (2) that showed significant expression changes after CK treatment ($P < 0.001$, Figure 1D). Among them, *CYTOKININ-RESPONSIVE GATA FACTOR1* (*CGA1*) and cytokinin response factor2/5 have been previously characterized in the context of CK responses (Rashotte et al., 2006; Kollmer et al., 2011), while *MYB34* regulates indolic glucosinolate biosynthesis (Celenza et al., 2005; Frerigmann and Gigolashvili, 2014). *MYB14* also functions in cold tolerance

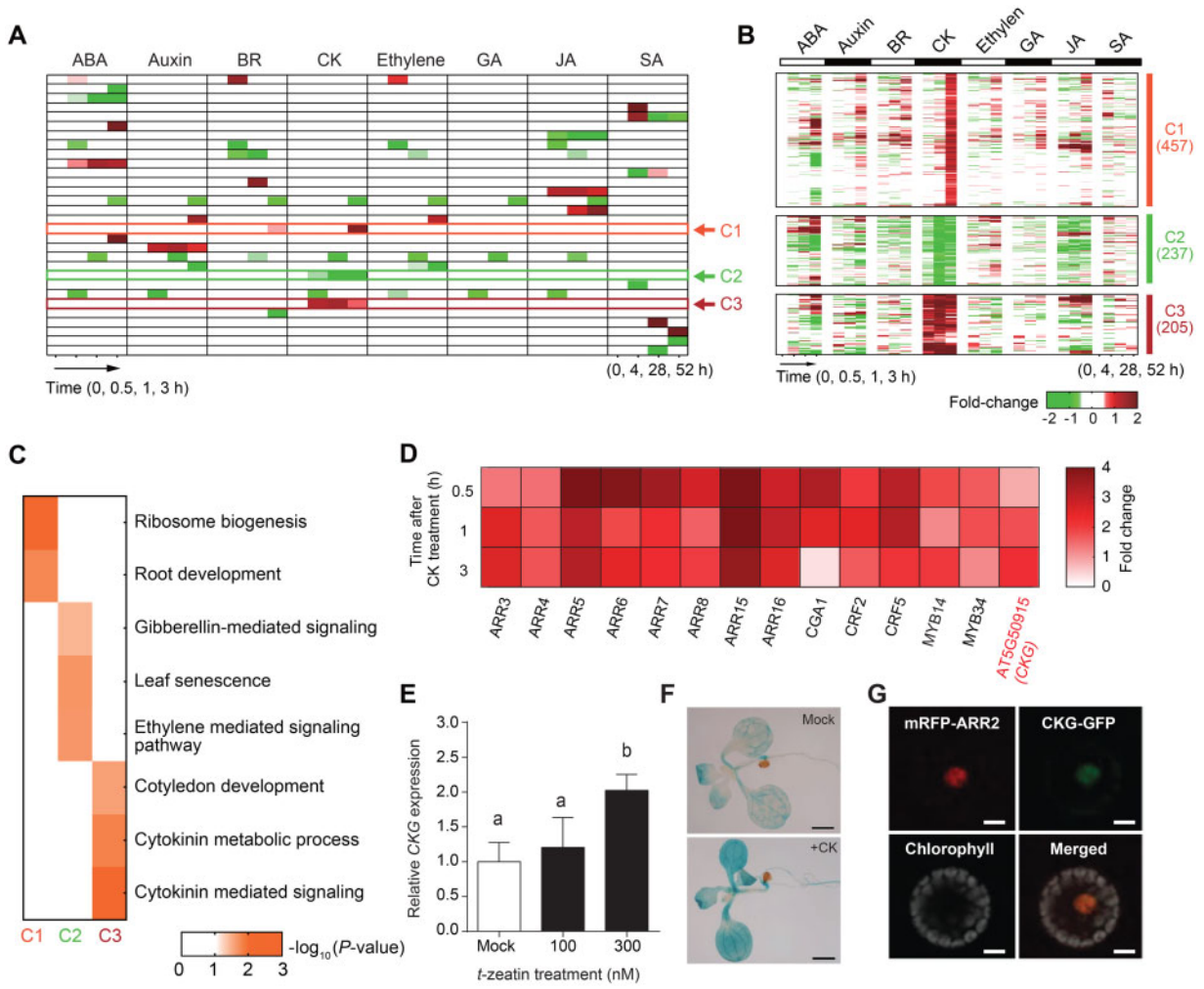

Figure 1 Transcriptome-wide discovery of potential CK signaling regulators. A, Differential gene expression patterns in hormone responses. Red and green colors indicate up- and downregulated gene expression, respectively, in time points under different hormone-treated conditions. ABA, abscisic acid; BR, brassinosteroid; GA, gibberellin; JA, jasmonic acid; SA, salicylic acid. B, The three clusters of gene expression patterns associated with CK response. Red and green indicate up- and downregulation in time points, respectively, under CK-treated conditions. Color bar, the gradient of $\log_2$(fold changes). C, Gene ontology biological processes represented by the genes in each cluster. Color bar, the gradient of $-\log_{10}$(*P*-values) from Fisher's exact test. D, Fourteen transcription factors in cluster 3 show the significant expression changes after CK treatment ($P < 0.001$). Color bar, the gradient of $\log_2$(fold changes). E, *CKG* expression was induced by CK in a dose-dependent manner. Seven-day-old seedlings were treated with or without CK for 30 min. The level of *CKG* expression in the absence of CK was set to 1, and its relative value is presented. Error bars, SD ($n = 3$). F, CK induced the expression of *pCKG:GUS* in seedlings. CK treatment, 300-nM *t*-zeatin for 1 h. Scale bar, 1 mm. G, CKG localizes in the nucleus. *35S:CKG-GFP* was co-transfected with *35S:mRFP-ARR2* as a nucleus marker. Scale bar, 10 μm. Different letters indicate significant differences at $P < 0.05$ based on Tukey's honestly significant difference (HSD) test.

by regulating the expression of *C-REPEAT/DRE BINDING FACTOR* (*CBF*) genes (Chen et al., 2013). However, the function of AT5G50915, hereafter named *CKG*, has not been characterized, and is the focus of this work.

To examine the potential role of CKG as a regulator or mediator of CK responses, we first confirmed the induction of *CKG* expression by CK treatment. In agreement with the transcriptome results, we observed that CKs did upregulate the expression of *CKG* in 7-d-old seedlings in a dose-dependent manner (Figure 1E). We also generated a promoter reporter line by placing the β-glucuronidase gene *GUS* under the control of the *CKG* promoter (*pCKG:GUS*). We detected strong GUS signal in cotyledons, root, leaves, ovules, vasculature, embryos, inflorescence, and flowers (Supplemental Figure S2A). GUS signal was further induced by CK treatment (Figure 1F). *CKG* is predicted to encode a member of the bHLH family of transcription factors (Toledo-Ortiz et al., 2003). To determine the subcellular localization of CKG, we fused the *CKG* coding sequence to the green fluorescent protein (*GFP*), and transfected Arabidopsis protoplasts with the resulting *35S:CKG–GFP* construct together with the nuclear marker gene *mRFP-ARR2* (encoding a fusion between ARR2, a transcription regulator of CK signaling, and the red fluorescent protein; Hwang and Sheen, 2001). The CKG–GFP fusion clearly co-localized with mRFP-ARR2 in the nucleus (Figure 1G). We further examined *CKG* expression in the CK signaling mutant *arr2* and a line overexpressing *ARR2*, as well as the CK degradation mutant *CKX2*, which degrades

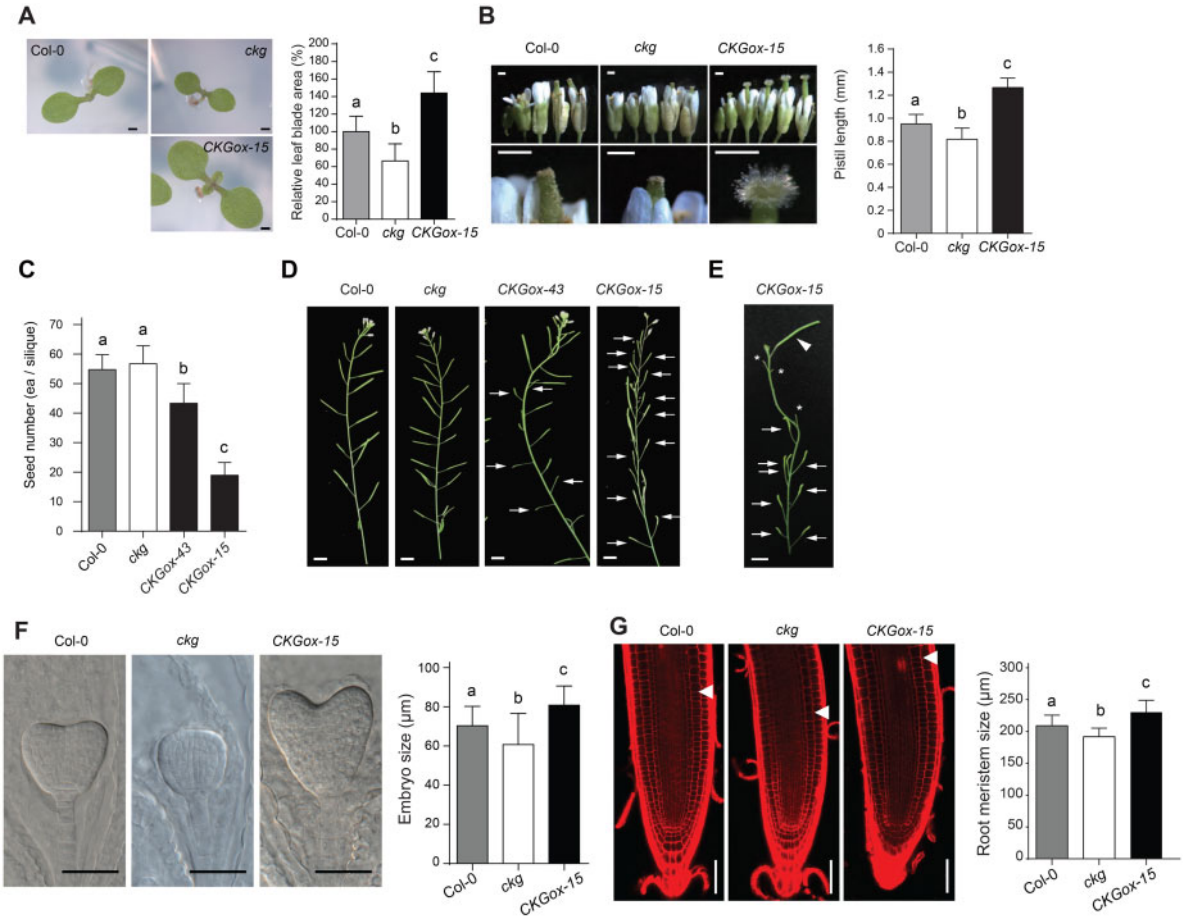

Figure 2 CKG promotes the growth of various organs at different developmental stages. A, (Left) representative cotyledons of Col-0, *ckg*-knockout, and *CKG*-overexpressing lines. Scale bar, 500 μm. (Right) Cotyledons of 7-d-old *CKGox-15* seedlings are larger than those of Col-0 by 40%, but *ckg* cotyledons are smaller than Col-0 by over 30%. Error bars, SD ($n \geq 35$). B, (Left) representative flowers of Col-0, *ckg*, and *CKGox-15* lines at serial developmental stages. In the *CKGox-15* line, pistils elongated fast, and stigma development was enhanced. Scale bars, 500 μm. (Right) pistils of the *CKGox-15* line were longer than those of Col-0, but the *ckg* mutant had shorter pistils at 2 d after pollination. Error bars, SD ($n = 6$). C, CKG affects the number of seeds. *CKGox* lines exhibited a low self-fertilization rate. Error bars, SD ($n = 30$). D, Alteration in fertilization by *CKG* expression levels affects silique development. *CKGox* lines had a portion of unfertilized siliques (arrows), and few siliques in the *CKGox-15* line were normally developed by natural fertilization. Scale bar, 5 mm. E, The normal development of siliques in the *CKGox-15* line after artificial pollination. Arrowheads indicate a pollinated silique, asterisks indicate stumps after cutting of peduncles, and arrows indicate unfertilized siliques. Scale bar, 5 mm. F, (Left) Representative embryos at the heart stage of Col-0, *ckg*, and *CKGox-15* lines. Scale bar, 50 μm. (Right) Embryos of the *CKGox-15* line at 4 d after pollination were larger than those of Col-0, but *ckg* embryos were smaller than Col-0 embryos. Error bars, SD ($n = 20$). G, (Left) Representative root tips of Col-0, *ckg* and *CKGox-15* lines. White arrowheads indicate the transition zone (TZ). Scale bar, 50 μm. Right; the sizes of root meristems in *ckg* and CKGox-15 lines were significantly reduced and increased compared to Col-0, respectively. Error bars, SD ($n = 12$). Different letters indicate significant differences at $P < 0.05$ based on Tukey's honestly significant difference (HSD) test

endogenous CK, overexpressing line (Werner et al., 2003). *CKG* was highly expressed regardless of the CK treatment in the type-B *ARR2*-overexpressing line compared to the wild-type Col-0, but the CK-responsive induction of *CKG* expression was hampered in the *arr2* mutant and the *CKX2*-overexpressing line (Supplemental Figure S2B). We then turned to a protoplast reporter assay using *pARR6:LUC* as a readout for CK signaling (Hwang and Sheen, 2001). Overexpression of *CKG* increased transcriptional activation of the *ARR6* promoter, and this effect was further enhanced by treatment with CK (Supplemental Figure S2C). These results indicate that CKG may function as a mediator of a canonical CK signaling cascade.

CKG enhances the growth of various organs

To further unravel the biological function of CKG, we generated lines overexpressing *CKG* and selected two individual lines with high *CKG* expression (Supplemental Figure S3C). We also identified a loss-of-function allele of CKG: the T-DNA insertion line SALK_141414C named *ckg*, which has severely reduced *CKG* transcript levels and is therefore considered a null allele (Supplemental Figure S3, A and C). Seedlings of the *CKGox-15* line, with the highest *CKG* expression level, showed larger cotyledons compared to Col-0, while the *ckg* mutant had smaller cotyledons (Figure 2A). Indeed, cotyledon size of 7-d-old seedlings increased by over 40% in *CKGox-15* seedlings, but decreased by 30% in the *ckg* mutant, relative to Col-0.

Since we had observed high *pCKG:GUS* signal in flowers (Supplemental Figure S2A), we paid close attention to any phenotype in reproductive structures and measured pistil length in all genotypes. Arabidopsis undergoes self-pollination (autogamy) by promoting the growth of the pistil through a circle of stamens shortly after flower buds open. Pistils from *CKGox-15* flowers outgrew the stamen at an earlier stage and were longer than Col-0, whereas *ckg* flowers had slightly shorter pistils (Figure 2B). The outgrowth of pistils in *CKG*-overexpressing lines resulted in individual siliques with fewer seeds (Figure 2C). In addition, the *CKGox-15* line formed many aborted siliques that contained few seeds (Figure 2D). However, the *CKGox-15* line was fully fertile, as hand pollination restored normal seed set (Figure 2E).

CKG is expressed in the egg cell and central cells (Johnston et al., 2007), and in the embryo (Supplemental Figure S2A), which suggests that CKG functions in early ovule and embryo development. Developing seeds of the *CKGox-15* line exhibited larger embryos at 4 d after pollination compared to Col-0 and the *ckg* mutant (Figure 2F). We also observed that most radicles of *CKGox-15* embryos were bent and skewed within the seed, which is likely due to enhanced outgrowth of the cotyledons and embryonic root within a limited space. A fraction of *ckg* mutant embryos showed a defective and abnormal development not seen in Col-0 or the *CKGox-15* line (Supplemental Figure S4). In addition to alterations in reproductive structures, ectopic expression of *CKG* in the overexpression lines increased the size of root meristems compared to Col-0, while the *ckg* mutant showed smaller root meristems (Figure 2G), which indicates that CKG may drive early cell elongation or differentiation in the root meristem. We also generated a *CKG* deletion line with clustered regularly interspaced short palindromic repeats (CRISPR)/CRISPR-associated protein 9 (Cas9), named *CKG-CAS9* (Supplemental Figure S3, A and B). *CKG-CAS9* plants showed a similar phenotype as the *ckg* mutant—short pistil length, and smaller cotyledons, embryo, and root meristem compared to Col-0 (Supplemental Figure S5).

The visible phenotypes associated with variation in *CKG* levels therefore point to cell and organ growth as a CK response, leading us to hypothesize that cell cycle progression and cell expansion might be directly under the control of CKG.

CKG regulates cell cycle and macromolecule synthesis genes

To test whether genes related to cell cycle progression and cell expansion were regulated by *CKG*, we used microarrays to profile transcript levels in the cotyledons of 7-d-old Col-0 and *ckg* seedlings. We identified differentially expressed genes (DEGs) in *ckg* relative to Col-0, based on an absolute fold-change of 1.5 or more and with an associated $P < 0.05$. Among the DEGs, 755 genes and 549 genes were up- and downregulated, respectively (Figure 3A; Supplemental Figure S6 and Supplemental Data Set S1).

To investigate the biological processes related to these DEGs, we determined the GO terms that were enriched in the DEGs that were up- and downregulated using BiNGO (Maere et al., 2005; Figure 3B; Supplemental Data Set S2). Interestingly, downregulated DEGs in the *ckg* mutant showed strong enrichment with cell cycle- and organ growth-related biological processes ("DNA replication", "DNA conformation change", "regulation of cell cycle", and "nitrogen/amino acid metabolic process"). Upregulated DEGs in the *ckg* mutant included many genes associated with various stress responses ("response to salt/oxidative/light/temperature/biotic stress"). These results indicated that *CKG* likely regulates organ growth via the modulation of transcript levels for genes involved in cell cycle progression and macromolecule synthesis.

We then tested whether CKG directly controlled the expression of the core cell cycle regulators (Menges et al., 2005; Gutierrez, 2009) that were downregulated in the *ckg* mutant by chromatin immunoprecipitation (ChIP) analysis using an anti-HA antibody on chromatin extracted from *35S:CKG-HA* transfected protoplasts. Since bHLH transcription factors are known to bind to the E-box motif (CANNTG; Heim et al., 2003), we looked for the E-box in the promoters of candidate genes and designed the relevant primer sets for ChIP analysis (Supplemental Figure S7 and Supplemental Table S1). Indeed, we observed direct binding of CKG to the promoters of *WEE1*, *DP-E2F-like 1* (*DEL1*), and the Arabidopsis homologue of yeast *CDC10 Target1a* (*CDT1a*; Figure 3C). In addition, CKG binding was highly enriched at the *ARR6* promoter regions. CKG binding was also highly enriched at the *CKG* promoter regions, suggesting that CKG reinforces its activity through a positive feedback loop to allow sufficient gene regulation. To test the stability of CKG protein, we transfected protoplasts with *35S:CKG-HA* and treated with/without CK (*t*-zeatin) and MG132, a 26S proteasome inhibitor with cycloheximide, a protein synthesis inhibitor. The protein level of CKG started to decrease in 10 min, and MG132 treatment delayed CKG degradation. CK did not affect the stability of CKG protein (Supplemental Figure S8).

To elucidate the genetic relationship between *CKG* and individual target genes during vegetative growth, we first monitored growth daily for the *ckg* mutant, *CKG* overexpressing lines, as well as selected mutants in target genes. *wee1* mutants in particular exhibited a retarded growth phenotype similar to that of the *ckg* mutant (Figure 3D). WEE1 is well conserved in eukaryotes and functions as a kinase controlling cell cycle progression during the S phase, especially under DNA replication stress (O'Connell et al., 1997; Kellogg, 2003). However, the other selected mutants did not show any visible phenotypes, which might be due to functional redundancy with related genes. Our data therefore suggest that CKG directly controlled *WEE1* expression to regulate cell growth downstream of CK signaling.

To test this hypothesis, we examined the induction of *WEE1* transcription by CKG using a protoplast reporter

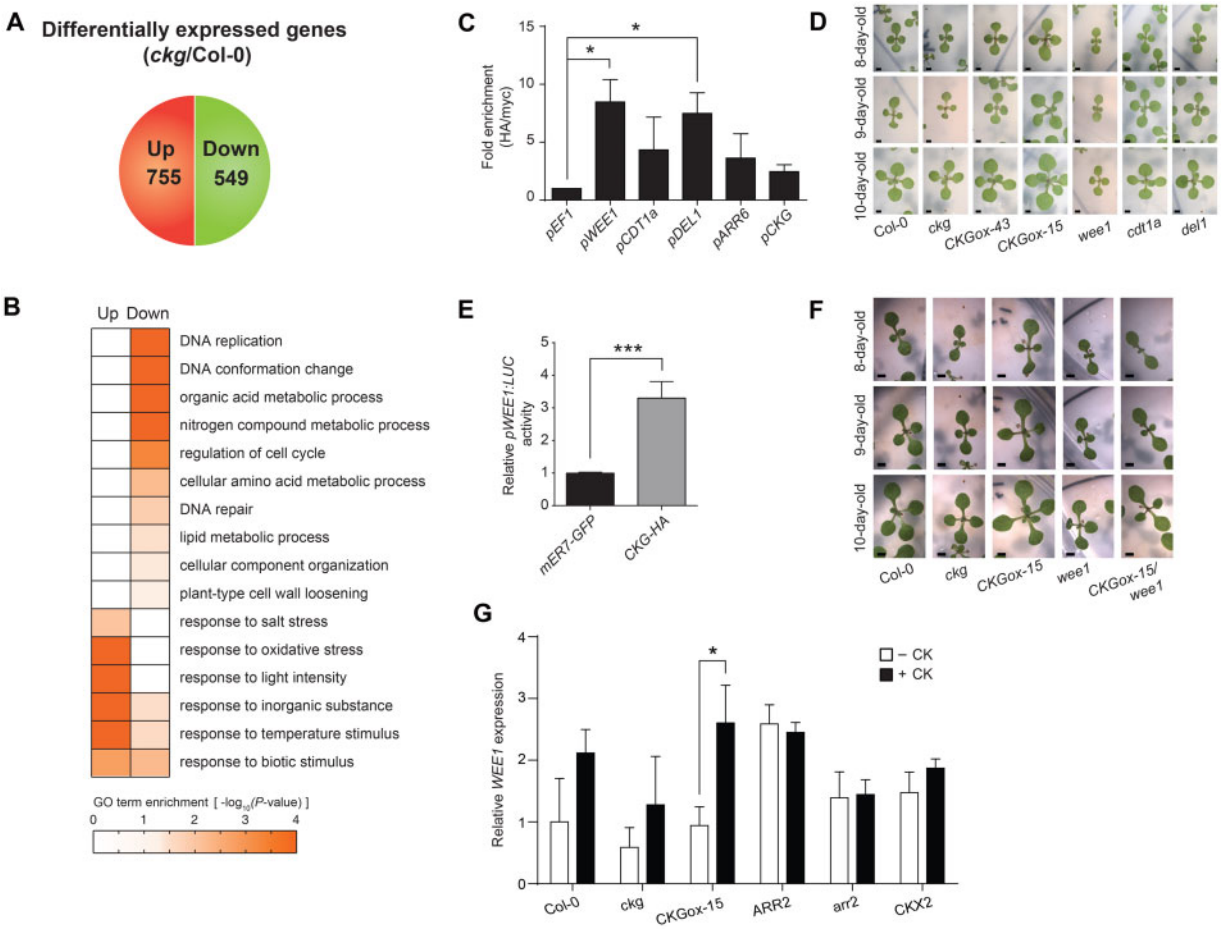

Figure 3 The downstream targets of CKG are mainly involved in the cell cycle and macromolecule synthesis. A, The number of up- and downregulated genes in the *ckg* mutant compared to Col-0. Among the genes with $P < 0.05$, those with $\log_2$(fold changes) > 0.58 and less than -0.58 were classified as the up- and downregulated genes, respectively. B, GO terms represented by the up- and downregulated genes in the *ckg* mutant. The downregulated genes were involved in cell cycle, DNA replication, and macromolecule metabolic processes, whereas the upregulated genes were mainly related to response to biotic and abiotic stresses. C, CKG directly binds to the promoters of core cell cycle regulators. Protoplasts were transfected with *35S:CKG-HA*, and ChIP assays of the designated promoters were performed with anti-HA antibody and anti-myc antibody as background. The *EF1* promoter was used as a negative control. Fold enrichment was measured by calculating the ratios between normalized results from anti-HA antibody and anti-myc antibody. Error bars, SD ($n = 3$). D, *ckg* and *wee1* mutants showed similar phenotypes in the cotyledon and leaf growth. *CKGox* lines grew faster than Col-0, but the *ckg* and *wee1* mutants were smaller than Col-0. The other mutants did not show a growth difference compared to Col-0. Scale bar, 1 mm. E, CKG increases *pWEE1:LUC* reporter activity. Protoplasts were transfected with *pWEE1:LUC* and *35S:CKG-HA*. *mER7-GFP* was used as a control and normalized to 1. Error bars, SD ($n = 4$). F, *CKGox-15/wee1* and *wee1* plants showed smaller leaves compared to Col-0. Scale bar, 1 mm. G, *WEE1* expression is induced by CKG in a CK-dependent manner. Seven-day-old seedlings of Col-0, *ckg*, *CKGox-15*, *ARR2*-overexpressing, *arr2*, and *CKX2*-overexpressing lines were treated with or without CK. The expression of *WEE1* was highly upregulated in the *CKGox-15* line after CK treatment, but not in the *arr2* and *CKX2*-overexpressing lines. The level of *WEE1* expression in Col-0 without CK was set to 1, and its relative value was presented. Error bars, SD ($n = 3$). CK treatment, 300-nM *t*-zeatin for 3 h. Asterisks indicate significant differences based on the *P*-value of two-tailed Student's *t* test (*< 0.05; **< 0.01; ***< 0.001)

assay. Co-transfection of *35S:CKG-HA* induced *pWEE1:LUC* promoter activity, confirming our assumptions (Figure 3E). As an independent genetic test, we crossed the *CKG* overexpressing line with the *wee1* mutant to determine the genetic hierarchy between CKG and WEE1. *CKGox-15/wee1* plants had the same retarded growth phenotype as the *wee1* mutant, placing WEE1 downstream of CKG (Figure 3F). We also measured *WEE1* expression levels in the *CKGox-15* line, the *ckg* mutant, and CK-related transgenic lines with or without CK treatment. *WEE1* expression was induced by CK treatment in the wild-type (Figure 3G) and was further enhanced in the *CKGox-15* line but disrupted in the *ckg* mutant. Although *WEE1* was highly expressed in the *ARR2* overexpressing line regardless of CK treatment, CK-dependent induction of *WEE1* was abolished in the *arr2* mutant and the *CKX2* overexpressing line. Collectively, these data suggest that CKG is a direct transcriptional regulator of *WEE1* during CK signaling.

CKG regulates cell growth and CK-mediated cell cycle transition independently of ploidy

To further unravel the function of CKG and WEE1 during cell growth, we measured the sizes of palisade cells in 7-d-old cotyledons and 8- to 10-d-old true leaves of the *ckg*

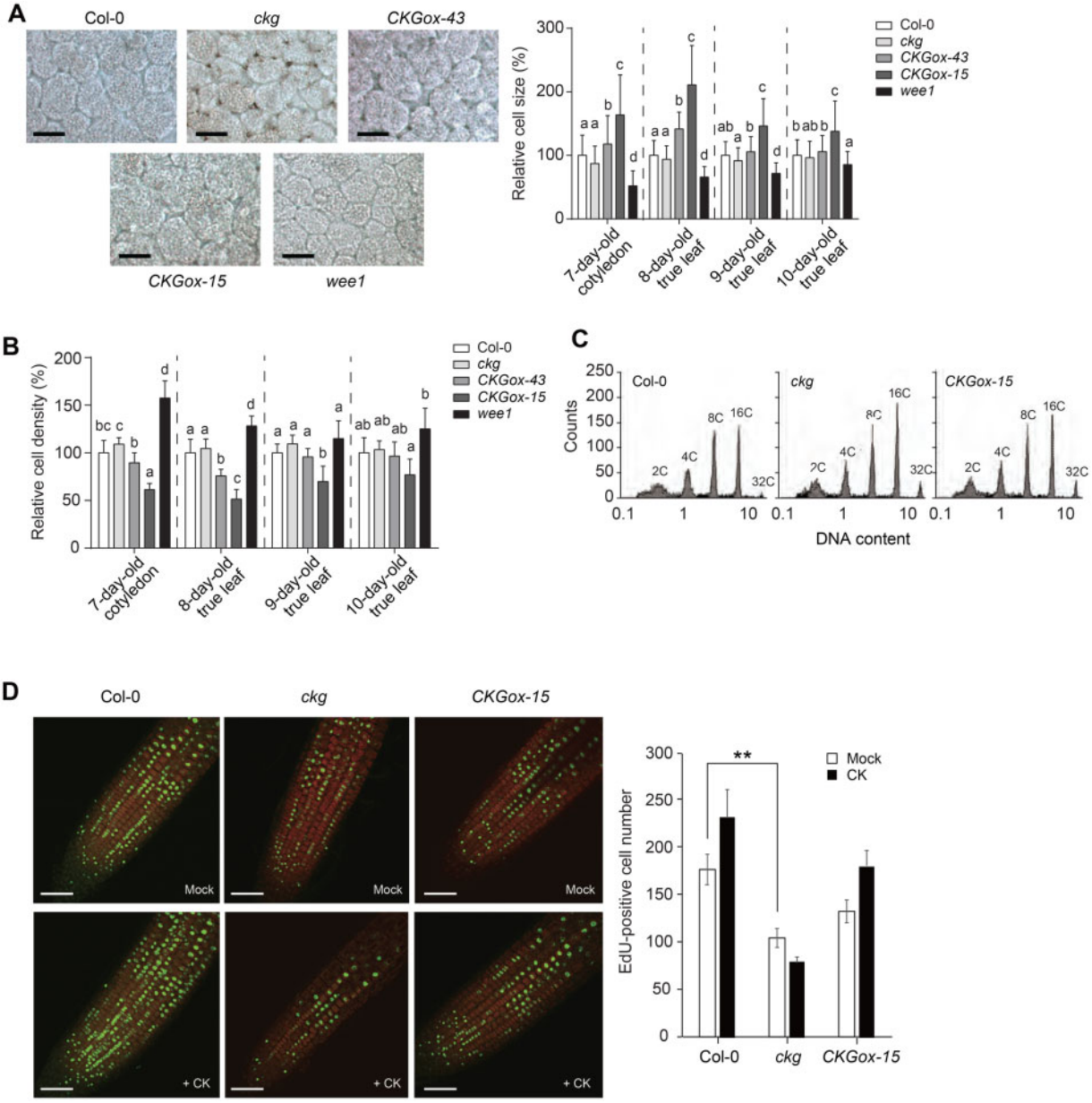

Figure 4 CKG functions as a growth regulator of cotyledons and leaves. A, (Left) Representative palisade cells of 7-d-old cotyledons of Col-0, *ckg*, *CKGox*, and *wee1* lines. Scale bar, 50 μm. (Right) Relative cell size of cotyledons and leaves of Col-0, *ckg*, *CKGox*, and *wee1* lines. The *ckg* and *wee1* mutations resulted in smaller cotyledon and leaf cells compared to Col-0, while *CKGox* lines exhibited larger cells. Error bars, SD ($n \geq 100$). B, Relative cell densities of cotyledons and leaves at different growth stages. Due to the changes in cell size, cell densities of *CKGox* lines were low, but those of *ckg* and *wee1* mutants were relatively high throughout all growth stages. Error bars, SD ($n \geq 4$). C, The ploidy of Col-0, *CKGox-15*, and *ckg* plants was similar. Flow cytometric analysis was performed with 7-d-old cotyledons. D, S phase entries of mitotic cells in Col-0, *ckg*, and *CKGox-15* lines. S phase entries were visualized by EdU-staining of 6-d-old root tips. The seedlings were grown in the presence or absence of 100-nM *t*-zeatin, and then treated with EdU for 2 h. Scale bar, 50 μm. Error bars, SD ($n \geq 8$). Different letters indicate significant differences at $P < 0.05$ based on Tukey's honestly significant difference (HSD) test. Asterisks indicate significant differences based on the *P*-value of two-tailed Student's *t* test (*$P < 0.05$; **$P < 0.01$; ***$P < 0.001$)

mutant, the *CKGox* lines and the *wee1* mutant. The *CKGox* lines displayed larger cells, whereas the *ckg* mutant exhibited smaller cells relative to Col-0 (Figure 4A). The sizes of palisade cells in the *wee1* mutant were smaller than those of both Col-0 and the *ckg* mutant. These results suggest that CKG and WEE1 affect cell expansion in a similar fashion. While CKG had a profound effect on leaf growth at early growth stages, mature leaves from the *CKGox* lines and the *ckg* mutant were much closer in size and shape to those of Col-0 (Supplemental Figure S9). In addition, the *CKGox-15* line had an early flowering phenotype, which may be due to a shortened vegetative phase by a developmental and growth promotion during early growth stages (Supplemental Figure S10). In agreement with cell size, the

cotyledons and leaves of the *CKGox* lines, especially *CKGox-15*, had a lower cell density compared to Col-0, while the *ckg* and *wee1* mutants exhibited higher cell densities (*CKGox-15:* 39% decrease over Col-0; *ckg*: 9% increase over Col-0; *wee1*: 57% increase over Col-0; Figure 4B 7-d-old cotyledon).

Since cell size is largely related to ploidy levels, we measured DNA content contained in the nuclei of 7-d-old cotyledons for all genotypes. However, we failed to observe notable changes in ploidy for the *CKGox-15* line or the *ckg* mutant when compared to Col-0 (Figure 4C). Similarly, the *wee1* mutation did not affect ploidy levels, as expected (De Schutter et al., 2007). Therefore, CKG and WEE1 regulate cell expansion in a ploidy-independent manner. Finally, we tested whether CKG was involved in cell cycle transitions under the control of CKs by monitoring 5-ethynyl-2′-deoxyuridine (EdU) incorporation into the nuclei of 6-d-old seedlings that are undergoing DNA replication and thus have entered the S phase (Kotogány et al., 2010). The number of EdU-positive cells was significantly lower in the *ckg* mutant relative to Col-0, but remained unchanged in the *CKGox-15* line (Figure 4D). The number of EdU-positive cells rose in response to CK treatment in Col-0, but not in the *ckg* mutant (Figure 4D). Our data therefore support the hypothesis that CKG mediates the G1/S transition during cell cycle progression as well as cell cycle speed during root growth in response to CKs.

Discussion

Identification of a novel transcription factor involved in CK-mediated regulation of cell size and cell cycle progression

We exploited a microarray data set cataloging plant responses to various phytohormones to identify transcriptional regulators specific for CKs. Our analysis revealed multiple candidate genes, several of which had been previously described as being involved in CK signaling, thus validating our approach. We named another CK-specific gene *CKG* (for *CYTOKININ-RESPONSIVE GROWTH REGULATOR*) and focused on its characterization. *CKG* transcript levels were induced by CK treatment, and *CKG* overexpression led to the activation of transcription from the *pARR6:LUC* reporter, positioning CKG downstream of CK perception and identifying it as a positive factor along the CK signaling cascade. A phenotypic analysis of *CKG*-overexpressing lines alongside a loss-of-function mutant demonstrated that CKG increases cell size, plant growth rates and entry into the S phase of the cell cycle. In sum, CKG is a key regulator participating in cell growth and cell cycle regulation in response to CK.

CK responses in cell growth regulation are complicated because of their opposite actions in the SAM and the RAM. To explain these diametrically opposed features of CK signaling, many reports have proposed the presence of cell- and tissue-specific regulators of CK signaling (reviewed in Takahashi et al., 2013; Zhang et al., 2013; Schaller et al., 2014). Moreover, CKs are connected to auxin signaling, as ARR1 and ARR12 upregulate *SHORT HYPOCOTYL2* (*SHY2*) expression, which itself minimizes auxin transport by repressing the expression of the auxin transporters *PIN-FORMED* (*PIN*) and related genes. This modulation of auxin transport controls root meristem size by affecting the balance between the rates of cell proliferation and differentiation (Ioio et al., 2008; Moubayidin et al., 2010). Moreover, CK and auxin interact for the regulation of SAM activity via MONOPTEROS (MP, also known as AUXIN RESPONSE FACTOR5 or ARF5), which represses *ARR7* and *ARR15* expression in the central zone (Zhao et al., 2010). However, the roles of CKs in root cell proliferation cannot be easily summarized by a linear signaling pathway, as CKs affect each growth stage and tissue differently. Other phytohormones such as jasmonic acid, abscisic acid, strigolactones, gibberellins, ethylene, and brassinosteroids are also involved in the regulation of the cell cycle, but their signal integration is largely unknown (Del Pozo et al., 2005; reviewed in Vanstraelen and Benková, 2012; Takatsuka and Umeda, 2014). In addition, CK levels can affect the size of the root meristem. The transcription factor PHABULOSA (PHB) induces CK biosynthesis in the distal parts of the root meristem, which results in the activation of ARR1 in the elongation/differentiation zone, where ARR1 then represses both *PHB* and the microRNA *MIR165A*, a negative regulator of PHB, thereby forming an incoherent regulatory loop that controls meristem size (Dello Ioio et al., 2012). Another level of regulation comes from the oscillation of endogenous CK contents as a function of the cell cycle, during which CKs mainly accumulate during the S and M stages (Redig et al., 1996). Hartig and Beck (2005) also presented evidence for the accumulation of CKs at stage transitions such as the G1/S and the M/G1 transitions. Hartig and Beck proposed that the transient peak in CK levels and low CK content at the end of each phase were equally important for cell cycle stage transitions. Overall, the regulation of the cell cycle by CKs should be considered holistically by integrating CK-responsive factors with the target tissue or cell type, cell cycle stage and signaling from other phytohormones.

Menges et al. (2005) profiled the transcriptome of a synchronized MM2d Arabidopsis cell line over the course of the cell cycle. They reported that *CKG* expression was constant over all cell cycle stages, although CKG target genes (*WEE1*, *CDT1a*, and *DEL1*) were induced at specific stages, which suggests that the regulation of *CKG* expression and its targets is distinct and reflects the stage of the cell cycle. In addition, several bHLH proteins form homo- or heterodimers in mammals, in the fruit fly (*Drosophila melanogaster*; Evan and Littlewood, 1998), and in plants (Halliday et al., 1999; Lingam et al., 2011; Liu et al., 2013). The potential for combinatorial dimerization may result in the observed distinct transcriptional profiles (Heim et al., 2003). Likewise, CKG may interact with other factors that are themselves cell cycle stage-specific, a notion that is supported by the fact that CKG protein has a short half-life

(Supplemental Figure S4). Therefore, CKG may coordinate cell cycle-related genes together with other transcription regulators that respond to various signals, including CKs, to promote entry into the S phase of the cell cycle.

CKG regulates cell size

CKs induce *CKG* expression, which in turn regulates the expression of cell cycle genes and various macromolecular synthesis genes. CKG physically binds to promoters of cell cycle-promoting factors such as *WEE1*, *CDT1a*, and *DEL1*, consistent with a role for CKG in cell cycle regulation in response to CK signaling. Although we failed to observe any significant differences in leaf size in *cdt1a* or *del1* mutants relative to Col-0 (Figure 3D), we hypothesize that redundancy may partially mask their contribution to cell cycle progression and cell division. Indeed, *DEL1* has two closely related genes in the Arabidopsis genome, while yeast *CDT1* has two Arabidopsis homologs. In contrast, the *wee1* mutant exhibited smaller cell size in cotyledons when compared to the wild-type Col-0 and also showed delayed growth. The WEE1 kinase is a cell cycle checkpoint that measures DNA damage and cell size at the G2/M transition (O'Connell et al., 1997; Kellogg, 2003), so we had expected to see cell division and endoreduplication phenotypes in the *wee1* mutant. Transgenic lines overexpressing *WEE1* showed no significant differences in cell size, although limited overexpression of *WEE1* using a heat shock-inducible system resulted in cell enlargement (De Schutter et al., 2007), which resolved the function of WEE1 in the promotion of cell expansion. However, ploidy levels remained normal in various tissues from *wee1* plants (De Schutter et al., 2007), which fits well with the absence of ploidy changes in *CKG* gain- and loss-of-function lines and indicates that CKG and WEE1 may not affect endoreduplication or DNA volume and thus increase cell size independently of ploidy levels. *WEE1* expression is also induced by DNA damage by the two upstream kinases ATAXIA-TELANGIECTASIA MUTATED (ATM) and ATM AND RAD3-RELATED (ATR). There is little evidence to suggest that WEE1 may participate in cell size increase. Therefore, even though we can firmly link CKG and WEE1 in the control of cell size, we cannot exclude the existence of an additional player that regulates cell size and that would act downstream of CKG but upstream of WEE1. We do note that the ploidy-independent cell size increase observed here may be partially explained by enhanced macromolecule synthesis, as pointed out by our transcriptome analysis.

Although ploidy level is a major factor controlling cell size, other ploidy-independent factors control cell size as well, for instance, the level of cellular vacuolization or the induction of genes involved in macromolecule biosynthesis (reviewed in Sugimoto-Shirasu and Roberts, 2003). It is worth noting that the expression of genes related to macromolecule biosynthesis is reduced in the *ckg* mutant, which suggests that changes in cell size reflect macromolecule biosynthesis potential. Like other cellular events, cell growth needs to be accompanied by the production of macromolecules such as nucleic acids, proteins, carbohydrates, and lipids to sustain growth. In particular, macromolecules such as cellulose and phospholipids are essential structural components for cell wall expansion and the addition of new membrane at the plasma membrane, endomembrane systems, and organelles.

The effect of ploidy on cell size can be easily explained by the resulting increase in gene dosage, but cannot explain how CKG affects cellular growth. Instead, CKG may specifically induce the expression of genes related to cell growth, resulting in larger cells without resorting to ploidy changes. The finding that overexpression of *CKG* later during plant development is not accompanied by changes in overall plant size also suggests that CKG-mediated effects on cell growth are somewhat restricted and do not go over a pre-determined growth promotion threshold.

In this work, we propose that CKG is a key transcription factor controlling cell cycle regulators to increase organ size and growth rates in a ploidy-independent manner. CKG is a mediator of a canonical CK signaling cascade, mainly downstream of a type-B ARR2, connecting to WEE1 in the control of cell size and cycle (Supplemental Figure S11). It is of note that CK, however, still induces *CKG* expression in the *arr2* mutant (Figure S2B), suggesting that other type-B ARRs may play a role in CK-mediated *CKG* expression. However, the exact nature of the regulatory mechanisms behind CKG-mediated cell and organ growth remain to be fully investigated. For example, how does CKG regulate the progression through cell cycle stages and what are its co-regulators? What other factors does CKG interact with to modulate gene expression? It will be informative to study how CKG is connected to other known cell growth regulators that are under the control of CKs. In addition, CKG affects cell size regulation at an early growth and development stage, which might constitute a useful trait that can be harnessed to promote growth, early flowering, and higher productivity of leaf vegetables.

Methods

Plant materials and growth conditions

Arabidopsis thaliana accession Col-0 was used as the wild-type control and as the genetic background of the transgenic lines. The plants were grown in a controlled growth chamber (23°C, 16-h light/8-h dark). T-DNA insertion lines of *ckg* (SALK_141414C), *wee1* (SALK_039890C), *cdt1a* (GABI_025G08), *del1* (SALK_105648), and *arr2* (SALK_016143) were provided by the Arabidopsis Biological Resource Center. The *ARR2* and *CKX2* overexpression lines were previously described (Choi et al., 2010). Plants for protoplast isolation were grown in short-day conditions (23°C, 10-h light/14-h dark). To generate transgenic plants overexpressing *CKG-HA*, the *CKG* coding sequence was cloned into the pCB302ES vector containing the CaMV 35S promoter and a HA epitope tag. The expression level of *CKG* was verified by reverse transcription quantitative polymerase chain reaction (RT-qPCR) using a *CKG*-specific primer set and also by western blot with a horseradish peroxidase-conjugated

high-affinity anti-HA antibody (1:2,000, Anti-HA-Peroxidase, High Affinity, Roche, catalogue no. 12013819001). To generate *pCKG:GUS* transgenic plants, a 2-kb sequence of the *CKG* promoter was cloned into pCAMBIA1303. The primers used for cloning are listed in Supplemental Table S2.

RT-qPCR analysis

Total RNA was isolated using TRIzol reagent (Invitrogen) according to the manufacturer's manual. One microgram of total RNA was used to synthesize cDNA using oligo(-dT) primers and ImProm-II reverse transcriptase (Promega). RT-qPCR was performed with gene-specific primers (*CKG*, *WEE1*) with the Light Cycler 2.0 (Roche) and the SYBR Premix Ex Taq system (Takara). *EUKARYOTIC TRANSLATION INITIATION FACTOR 4A1* (*EIF4A1*) was used as an internal control. The primers used for RT-qPCR are listed in Supplemental Table S2.

Plasmid constructs and protoplast transient expression assay

The full-length cDNA of *CKG* was cloned into plant expression vectors containing the CaMV 35S promoter and an HA epitope tag. For the reporter assay, 2×10^4 protoplasts were transfected with 20 μg of total plasmid DNA composed of different combinations of the reporters (*pARR6:LUC*, *pWEE1:LUC*), effector (*35S:CKG-HA*), and an internal control (*mER7-GFP*). For the *pARR6:LUC* reporter assay, transfected protoplasts were incubated for 3 h and then treated with 100-nM *t*-zeatin for 3 h at room temperature. To confirm the subcellular localization of CKG, a *CKG–GFP* fusion construct was co-transfected with the *mRFP-ARR2* construct in protoplasts and observed with a confocal microscope (LSM800, Carl Zeiss). *pARR6:LUC*, *mRFP-ARR2*, and *mER7-GFP* constructs were previously described (Hwang and Sheen, 2001; Ryu et al., 2007; Choi et al., 2010). The primers used for cloning are listed in Supplemental Table S2.

CKG deletion by CRISPR-Cas9

Protospacer oligos targeting *CKG* were designed from http://crispr.hzau.edu.cn/CRISPR2/ (Liu et al., 2017) and cloned as described by (Schiml et al., 2016). Briefly, two protospacer oligos targeting *CKG* were inserted into each BbsI-digested pEn_C1.1. The sgRNA 1 containing first protospacer oligos from pEn_C1.1 was inserted into pDe-CAS9 by Bsu36I and MluI digestion and ligation. The sgRNA 2 containing second protospacer oligos from pEn_C1.1 was inserted into pDe-CAS9 containing sgRNA 1 by Gateway Cloning LR reaction, generating pDe-CAS containing both sgRNA 1 and 2. This construct was transformed in Col-0. The region surrounding the protospacer oligo target site was amplified from genomic DNA and inserted into pGEM-T Easy Vector. Targeted gene deletions were detected by sequencing of the pGEM-T Easy Vector containing amplified PCR products. The primers used for protospacer oligos and confirmation of *CKG* deletion are listed in Supplemental Table S2.

GUS staining

For determination of *CKG* expression, Arabidopsis samples were stained with GUS-staining buffer (100-mM Tris–HCl (pH 7.0), 2-mM ferricyanide, and 1 mM X-Gluc (5-bromo-4-chloro-3-indolyl-β-D-glucuronidase)) for 3 h. For the *CKG* induction experiment by CK treatment, the seedlings were transferred to 1/2 B5 medium with or without 300-nM *t*-zeatin and incubated for 3 h, and then observed with a stereomicroscope and a microscope (Axioplan2, Carl Zeiss).

Phenotypic analysis

For analysis of cotyledons and rosette leaves, seedlings were grown on 1/2 B5 medium (Duchefa) containing 1% sucrose (w/v; Duchefa) and 0.8% type-M agar (w/v; Sigma) at 23°C with a 16-h light/8-h dark photoperiod. As previously described with minor modifications (Jun et al., 2013), cotyledons and leaves were fixed with fixation solution (2.5% acetic acid (v/v), 2.5% formaldehyde (v/v), and 45% ethanol (v/v) in water) under a vacuum, and the size of palisade cells in the region between the mid-vein and leaf margin in the center of the leaf were measured using a microscope (Axioplan2, Carl Zeiss) and ImageJ software (NIH Image). Pistil lengths were measured at 2 d after pollination using a microscope (Axioplan2, Carl Zeiss). For analysis of embryos, developing seeds at 4 d after pollination were dissected under a stereomicroscope, and embryo sizes were measured using a microscope (Axioskop2, Carl Zeiss). To analyze root meristem size, sample preparations were performed as previously described (Malamy and Benfey, 1997), and measured using a confocal microscope (LSM800, Carl Zeiss).

Microarray

For microarray gene expression analysis, two independent biological replicates for Col-0 and three independent biological replicates for *ckg* cotyledons were analyzed with the Arabidopsis V4 Oligo Microarray (Agilent) according to the standard Agilent protocols. The total RNA integrity was measured by using the Bioanalyzer 2100 (Agilent). Fluorescent signals (probe intensities) were scanned using the Agilent microarray scanner. Log_2-intensities of whole samples were normalized using quantile normalization (Bolstad et al., 2003). To identify DEGs between two conditions, P-values were computed as previously described (Chae et al., 2013): (1) we computed *t*-statistics from the two-tailed *t* test for individual genes with assumption of unequal variance. Log_2(median differences) were computed for individual genes; (2) empirical null distribution of the *t*-statistics and log_2(median difference) was derived from random permutations of whole samples; (3) *P*-values of *t* test and log_2(-median difference) were computed based on corresponding empirical null distribution ; and (4) two *P*-values were integrated by Liptak–Stouffer's Z method (Hwang et al., 2005). DEGs were selected if they showed an over 1.5-fold change and $P < 0.05$. Microarray data were deposited in NCBI Gene Expression Omnibus (accession ID: GSE131029).

Functional enrichment analysis

BiNGO was used to identify GO biological processes significantly represented in DEGs (Maere et al., 2005). We used Benjamini and Hochberg false discovery rate corrected *P*-value provided from BiNGO to compute the enrichment *P*-value.

Chromatin immunoprecipitation

Chromatin immunoprecipitation (ChIP) assays were performed as previously described with minor modifications (Lee et al., 2007; Cho et al., 2014). Protoplasts were transfected with 20 μg of *35S:CKG-HA* constructs. After 6 h, protoplasts were crosslinked with 1% formaldehyde (v/v) for 10 min and quenched with 125-mM glycine. Harvested protoplasts were ground and resuspended with nuclei isolation buffer (0.25-M sucrose, 15-mM 1,4-piperazinediethanesulfonic acid (PIPES) (pH 6.8), 5-mM $MgCl_2$, 60-mM KCl, 15-mM NaCl, 1-mM $CaCl_2$, 1% Triton X-100 (v/v), and 1-mM phenylmethylsulphonyl fluoride). The nuclear pellets were resuspended in nuclei lysis buffer (50-mM 2-[4-(2-hydroxyethyl)piperazin-1-yl]ethanesulfonic acid (HEPES) (pH 7.0), 150-mM NaCl, 1-mM ethylenediaminetetraacetic acid (EDTA), 1% sodium dodecyl sulfate (SDS) (w/v), 1% Triton X-100 (v/v), 1-mM phenylmethylsulphonyl fluoride, and 1X Protease inhibitor cocktail for plant cell and tissue extracts (Sigma)). The chromatins were isolated and sheared by sonication to produce 0.5–1-kb DNA fragments. Chromatin fractions were diluted tenfold with nuclei lysis buffer and precleared with protein G agarose/salmon sperm DNA (Millipore) for 2 h at 4°C. The protein–DNA complexes were immunoprecipitated with anti-HA antibody (1:1,000, anti-HA tag antibody – ChIP Grade, Abcam, catalogue no. ab9110) and anti-myc antibody (1:1,000, Myc-Tag (9B11) Mouse mAb, Cell Signaling Technology, catalogue no. 2276) for 9 h at 4°C and further incubated with protein G agarose/salmon sperm DNA for 2 h at 4°C. After washing with low salt buffer (150-mM NaCl, 20-mM Tris–HCl (pH 8.0), 0.2% SDS (w/v), 0.5% Triton X-100 (v/v), and 2-mM EDTA) for 5 min at 4°C and high-salt buffer (500-mM NaCl, 20-mM Tris–HCl (pH 8.0), 0.2% SDS (w/v), 0.5% Triton X-100 (v/v), and 2-mM EDTA) for 5 min at 4°C, the immunocomplexes were eluted twice by elution buffer (0.5% SDS (w/v) and 0.1-M $NaHCO_3$) and then reverse crosslinked with 200-mM NaCl for 6 h at 65°C. After removing proteins with proteinase K, DNAs were purified by phenol–chloroform extraction and recovered by ethanol precipitation. Precipitated DNAs were resuspended with TE buffer (10-mM Tris–HCl (pH 8.0) and 1-mM EDTA) and used as qPCR templates with ChIP primer sets (Supplemental Table S2).

Ploidy analysis

Ploidy levels were measured using the ploidy analyzer PA-I (Partec) as described previously (Sugimoto-Shirasu et al., 2002). At least 7,000 nuclei isolated from cotyledons of 7-d-old seedlings were used for each ploidy measurement.

EdU staining

Six-day-old seedlings were treated with 1-μM EdU (Invitrogen Click-iT EdU Imaging Kit) for 2 h, transferred to fixative (4% formaldehyde (v/v)), permeabilized with 0.1% Triton X-100 (v/v) for 30 min and washed with 3% bovine serum albumin (BSA) (w/v) in phosphate-buffered saline (PBS). The seedlings were incubated in Click-iT reaction cocktail for 30 min in the dark, then washed with 3% BSA (w/v) in PBS three times before observation by confocal microscope (LSM510, Carl Zeiss).

Statistical analysis

Quantitative data were subjected to two-tailed Student's *t* tests or analysis of variance (ANOVA) test. For Student's *t* tests, asterisks indicate the *P*-values (*$<$ 0.05; **$<$ 0.01; ***$<$ 0.001). For ANOVA test, different letters indicate significant differences at $P < 0.05$ based on Tukey's honestly significant difference test.

Accession numbers

The sequence data from this article can be found in The Arabidopsis Information Resource (https://www.arabidopsis.org/) under the following accession numbers: ARR2 (AT4G16110), ARR6 (AT5G62920), CDT1a (AT2G31270), CKG (AT5G50915), CKX2 (AT2G19500), DEL1 (AT3G48160), EF1 (AT5G60390), EIF4A1 (AT3G13920), and WEE1 (AT1G02970).

Supplemental data

The following materials are available in the online version of this article.

Supplemental Figure S1. Expression patterns of representative genes in C1 and C2 cluster (related to Figure 1C).

Supplemental Figure S2. CK-dependent expression of *CKG* and its expression pattern in tissues.

Supplemental Figure S3. T-DNA insertion site and CRISPR-Cas9-meditated deletion site in *CKG*, and *CKG* expression levels in *ckg* and *CKGox* transgenic lines.

Supplemental Figure S4. Abnormal embryo growth in *CKGox*-15 and *ckg* plants.

Supplemental Figure S5. The *CKG-CAS9* deletion line shows similar phenotypes to the *ckg* mutant.

Supplemental Figure S6. PCA plot of Col-0 and *ckg* microarray samples.

Supplemental Figure S7. Promoter regions amplified for the ChIP assay in Figure 3C.

Supplemental Figure S8. CK does not affect the stability of CKG proteins.

Supplemental Figure S9. The growth phenotypes of *wee1*, *ckg*, and *CKGox* lines.

Supplemental Figure S10. The early bolting phenotypes of *CKGox-15* plants.

Supplemental Figure S11. Model of CK-mediated CKG action for the cell cycle.

Supplemental Data Set S1. List of DEGs related to Figure 3A.

Supplemental Data Set S2. Gene ontology of up- and downregulated genes in the *ckg* mutant.

Supplemental Table S1. CKG target gene candidates.

Supplemental Table S2. Primer list.

Acknowledgments

We are grateful to Professor Gyung-Tae Kim (Dong-A University, Korea) for the advice. We thank Hoyoung Nam for sample preparation.

Funding

This work was supported by the National Research Foundation of Korea (NRF) grant funded by the Korea government (MSIT) (2020R1A2C3012750).

Conflict of interest statement. Authors declare that they have no conflict of interest.

References

Arnaud D, Lee S, Takebayashi Y, Choi D, Choi J, Sakakibara H, Hwang I (2017) Cytokinin-mediated regulation of reactive oxygen species homeostasis modulates stomatal immunity in Arabidopsis. Plant Cell **29**: 543–559

Bartrina I, Otto E, Strnad M, Werner T, Schmülling T (2011) Cytokinin regulates the activity of reproductive meristems, flower organ size, ovule formation, and thus seed yield in Arabidopsis thaliana. Plant Cell **23**: 69–80

Bolstad BM, Irizarry RA, Astrand M, Speed TP (2003). A comparison of normalization methods for high density oligonucleotide array data based on variance and bias. Bioinformatics **19**: 185–193

Celenza JL, Quiel JA, Smolen GA, Merrikh H, Silvestro AR, Normanly J, Bender J (2005) The Arabidopsis ATR1 Myb transcription factor controls indolic glucosinolate homeostasis. Plant Physiol **137**: 253–262

Chae S, Ahn BY, Byun K, Cho YM, Yu M-H, Lee B, Hwang D, Park KS (2013) A systems approach for decoding mitochondrial retrograde signaling pathways. Science Signal **6**: rs4

Chen Y, Chen Z, Kang J, Kang D, Gu H, Qin G (2013) AtMYB14 regulates cold tolerance in Arabidopsis. Plant Mol Biol Rep **31**: 87–97

Cho, H., Ryu, H., Rho, S., Hill, K., Smith, S., Audenaert, D., Park, J., Han, S., Beeckman, T., Bennett, M.J., et al. (2014). A secreted peptide acts on BIN2-mediated phosphorylation of ARFs to potentiate auxin response during lateral root development. Nat Cell Biol **16**: 66–76

Choi D, Choi J, Kang B, Lee S, Cho YH, Hwang I, Hwang D (2014) iNID: an analytical framework for identifying network models for interplays among developmental signaling in Arabidopsis. Mol Plant **7**: 792–813

Choi J, Huh SU, Kojima M, Sakakibara H, Paek K-H, Hwang I (2010) The cytokinin-activated transcription factor ARR2 promotes plant immunity via TGA3/NPR1-dependent salicylic acid signaling in Arabidopsis. Dev Cell **19**: 284–295

Cortleven A, Leuendorf JE, Frank M, Pezzetta D, Bolt S, Schmülling T (2019) Cytokinin action in response to abiotic and biotic stresses in plants. Plant Cell Environ **42**: 998–1018

De Schutter K, Joubes J, Cools T, Verkest A, Corellou F, Babiychuk E, Van Der Schueren E, Beeckman T, Kushnir S, Inze D, et al. (2007). Arabidopsis WEE1 kinase controls cell cycle arrest in response to activation of the DNA integrity checkpoint. Plant Cell **19**: 211–225

Del Pozo JC, Lopez-Matas MA, Ramirez-Parra E, Gutierrez C (2005) Hormonal control of the plant cell cycle. Physiol Plant **123**: 173–183

Dello Ioio R, Linhares FS, Scacchi E, Casamitjana-Martinez E, Heidstra R, Costantino P, Sabatini S (2007) Cytokinins determine Arabidopsis root-meristem size by controlling cell differentiation. Curr Biol **17**: 678–682

Dello Ioio R, Galinha C, Fletcher AG, Grigg SP, Molnar A, Willemsen V, Scheres B, Sabatini S, Baulcombe D, Maini PK, et al. (2012). A PHABULOSA/cytokinin feedback loop controls root growth in Arabidopsis. Curr Biol **22**: 1699–1704

Dewitte W, Scofield S, Alcasabas AA, Maughan SC, Menges M, Braun N, Collins C, Nieuwland J, Prinsen E, Sundaresan V, et al. (2007). Arabidopsis CYCD3 D-type cyclins link cell proliferation and endocycles and are rate-limiting for cytokinin responses. Proc Natl Acad Sci **104**: 14537–14542

Evan G, Littlewood T (1998) A matter of life and cell death. Science **281**: 1317–1322

Frerigmann H, Gigolashvili T (2014) MYB34, MYB51 and MYB122 distinctly regulate indolic glucosinolate biosynthesis in Arabidopsis thaliana. Mol Plant **7**: 814–828

Gutierrez C (2009) The Arabidopsis cell division cycle. Arabidopsis Book **7:** e0120

Halliday KJ, Hudson M, Ni M, Qin M, Quail PH (1999) poc1: An Arabidopsis mutant perturbed in phytochrome signaling because of a T DNA insertion in the promoter of PIF3, a gene encoding a phytochrome-interacting bHLH protein. Proc Natl Acad Sci **96**: 5832–5837

Hartig K, Beck E (2005) Endogenous cytokinin oscillations control cell cycle progression of tobacco BY-2 Cells. Plant Biol **7**: 33–40

Heim MA, Jakoby M, Werber M, Martin C, Weisshaar B, Bailey PC (2003) The basic helix–loop–helix transcription factor family in plants: a genome-wide study of protein structure and functional diversity. Mol Biol Evol **20**: 735–747

Hejatko J, Ryu H, Kim GT, Dobesova R, Choi S, Choi SM, Soucek P, Horak J, Pekarova B, Palme K, et al. (2009). The histidine kinases CYTOKININ-INDEPENDENT1 and ARABIDOPSIS HISTIDINE KINASE2 and 3 regulate vascular tissue development in Arabidopsis shoots. Plant Cell **21:** 2008–2021

Higuchi M, Pischke MS, Mähönen AP, Miyawaki K, Hashimoto Y, Seki M, Kobayashi M, Shinozaki K, Kato T, Tabata S, et al. (2004). In planta functions of the Arabidopsis cytokinin receptor family. Proc Natl Acad Sci USA **101**: 8821–8826

Hwang D, Rust A, Ramsey S, Smith J, Leslie D, Weston A, de Atauri P, Aitchison J, Hood L, Siegel A, et al. (2005). A data integration methodology for systems biology. Proc Natl Acad Sci USA **102**: 17296–17301

Hwang I, Sheen J (2001) Two-component circuitry in Arabidopsis cytokinin signal transduction. Nature **413**: 383–389

Hwang I, Sheen J, Müller B (2012) Cytokinin signaling networks. Annu Rev Plant Biol **63**: 353–380

Ioio RD, Nakamura K, Moubayidin L, Perilli S, Taniguchi M, Morita MT, Aoyama T, Costantino P, Sabatini S (2008) A genetic framework for the control of cell division and differentiation in the root meristem. Science **322**: 1380–1384

Johnston A, Meier P, Gheyselinck J, Wuest S, Federer M, Schlagenhauf E, Becker J, Grossniklaus U (2007) Genetic subtraction profiling identifies genes essential for Arabidopsis reproduction and reveals interaction between the female gametophyte and the maternal sporophyte. Genome Biol **8**: R204

Jun S, Okushima Y, Nam J, Umeda M, Kim G-T (2013) Kip-related protein 3 is required for control of endoreduplication in the shoot apical meristem and leaves of Arabidopsis. Mol Cells **35**: 47–53

Kellogg DR (2003) Wee1-dependent mechanisms required for coordination of cell growth and cell division. J Cell Sci **116**: 4883–4890

Kieber JJ, Schaller GE (2014) Cytokinins. Arabidopsis Book **12:** e0168.

Kieber JJ, Schaller GE (2018) Cytokinin signaling in plant development. Development **145**: dev149344

Kim J (2016) CYTOKININ RESPONSE FACTORs gating environmental signals and hormones. Trends Plant Sci **21**: 993–996

Kollmer I, Werner T, Schmulling T (2011) Ectopic expression of different cytokinin-regulated transcription factor genes of Arabidopsis thaliana alters plant growth and development. J Plant Physiol **168**: 1320–1327

Kotogány E, Dudits D, Horváth GV, Ayaydin, F (2010) A rapid and robust assay for detection of S-phase cell cycle progression in plant cells and tissues by using ethynyl deoxyuridine. Plant Methods **6**: 5

Kurakawa T, Ueda N, Maekawa M, Kobayashi K, Kojima M, Nagato Y, Sakakibara H, Kyozuka J (2007) Direct control of shoot meristem activity by a cytokinin-activating enzyme. Nature **445**: 652–655

Lee JH, Yoo SJ, Park SH, Hwang I, Lee JS, Ahn JH (2007) Role of SVP in the control of flowering time by ambient temperature in Arabidopsis. Genes Dev **21**: 397–402

Leibfried A, To JPC, Busch W, Stehling S, Kehle A, Demar M, Kieber JJ, Lohmann JU (2005) WUSCHEL controls meristem function by direct regulation of cytokinin-inducible response regulators. Nature **438**: 1172–1175

Lingam S, Mohrbacher J, Brumbarova T, Potuschak T, Fink-Straube C, Blondet E, Genschik P, Bauer P (2011) Interaction between the bHLH transcription factor FIT and ETHYLENE INSENSITIVE3/ETHYLENE INSENSITIVE3-LIKE1 reveals molecular linkage between the regulation of iron acquisition and ethylene signaling in Arabidopsis. Plant Cell **23**: 1815–1829

Liu H, Ding Y, Zhou Y, Jin W, Xie K, Chen L-L (2017) CRISPR-P 2.0: an improved CRISPR-Cas9 tool for genome editing in plants. Mol Plant **10**: 530–532

Liu Y, Li X, Li K, Liu H, Lin C (2013) Multiple bHLH proteins form heterodimers to mediate CRY2-dependent regulation of flowering--time in Arabidopsis. Plos Genet **9**: e1003861

Mähönen AP, Bishopp A, Higuchi M, Nieminen KM, Kinoshita K, Törmäkangas K, Ikeda Y, Oka A, Kakimoto T, Helariutta Y (2006) Cytokinin signaling and its inhibitor AHP6 regulate cell fate during vascular development. Science **311**: 94–98

Maere S, Heymans K, Kuiper M (2005) BiNGO: a Cytoscape plugin to assess overrepresentation of gene ontology categories in biological networks. Bioinformatics **21**: 3448–3449

Malamy JE, Benfey PN (1997) Organization and cell differentiation in lateral roots of Arabidopsis thaliana. Development **124**: 33–44

Menges M, De Jager SM, Gruissem W, Murray JAH (2005) Global analysis of the core cell cycle regulators of Arabidopsis identifies novel genes, reveals multiple and highly specific profiles of expression and provides a coherent model for plant cell cycle control. Plant J **41**: 546–566

Moubayidin L, Perilli S, Dello Ioio R, Di Mambro R, Costantino P, Sabatini S (2010) The rate of cell differentiation controls the Arabidopsis root meristem growth phase. Curr Biol **20**: 1138–1143

Nishimura C, Ohashi Y, Sato S, Kato T, Tabata S, Ueguchi C (2004) Histidine kinase homologs that act as cytokinin receptors possess overlapping functions in the regulation of shoot and root growth in Arabidopsis. Plant Cell **16**: 1365–1377

Nishiyama R, Watanabe Y, Fujita Y, Le DT, Kojima M, Werner T, Vankova R, Yamaguchi-Shinozaki K, Shinozaki K, Kakimoto T, et al. (2011). Analysis of cytokinin mutants and regulation of cytokinin metabolic genes reveals important regulatory roles of cytokinins in drought, salt and abscisic acid responses, and abscisic acid biosynthesis. Plant Cell **23**: 2169

O'Connell MJ, Raleigh JM, Verkade HM, Nurse P (1997) Chk1 is a wee1 kinase in the G2 DNA damage checkpoint inhibiting cdc2 by Y15 phosphorylation. EMBO J **16**: 545–554

Poitout A, Crabos A, Petřík I, Novák O, Krouk G, Lacombe B, Ruffel S (2018) Responses to systemic nitrogen signaling in Arabidopsis roots involve *trans*-Zeatin in shoots. Plant Cell **30**: 1243

Raines T, Shanks C, Cheng C-Y, McPherson D, Argueso CT, Kim HJ, Franco-Zorrilla JM, López-Vidriero I, Solano R, Vaňková R, et al. (2016). The cytokinin response factors modulate root and shoot growth and promote leaf senescence in Arabidopsis. Plant J **85**: 134–147

Rashotte AM, Mason MG, Hutchison CE, Ferreira FJ, Schaller GE, Kieber JJ (2006) A subset of Arabidopsis AP2 transcription factors mediates cytokinin responses in concert with a two-component pathway. Proc Natl Acad Sci USA **103**: 11081–11085

Redig P, Shaul O, Inzé D, Van Montagu M, Van Onckelen H (1996) Levels of endogenous cytokinins, indole-3-acetic acid and abscisic acid during the cell cycle of synchronized tobacco BY-2 cells. FEBS Lett **391**: 175–180

Riou-Khamlichi C, Huntley R, Jacqmard A, Murray JAH (1999) Cytokinin activation of Arabidopsis cell division through a D-type cyclin. Science **283**: 1541–1544

Roitsch T, Ehneß R (2000) Regulation of source/sink relations by cytokinins. Plant Growth Regul **32**: 359–367

Ryu H, Kim K, Cho H, Park J, Choe S, Hwang I (2007) Nucleocytoplasmic shuttling of BZR1 mediated by phosphorylation is essential in *Arabidopsis* brassinosteroid signaling. Plant Cell **19**: 2749

Schaller GE, Street IH, Kieber JJ (2014) Cytokinin and the cell cycle. Curr Opin Plant Biol **21**: 7–15

Schiml S, Fauser F, Puchta H (2016) CRISPR/Cas-mediated site-specific mutagenesis in Arabidopsis thaliana using Cas9 nucleases and paired nickases. Methods Mol Biol **1469**: 111–122

Sugimoto-Shirasu K, Roberts K (2003) "Big it up": endoreduplication and cell-size control in plants. Curr Opin Plant Biol **6**: 544–553

Sugimoto-Shirasu K, Stacey NJ, Corsar J, Roberts K, McCann MC (2002) DNA topoisomerase VI is essential for endoreduplication in Arabidopsis. Curr Biol **12**: 1782–1786

Takahashi N, Kajihara T, Okamura C, Kim Y, Katagiri Y, Okushima Y, Matsunaga S, Hwang I, Umeda M (2013) Cytokinins control endocycle onset by promoting the expression of an APC/C activator in Arabidopsis roots. Curr Biol **23**: 1812–1817

Takatsuka H, Umeda M (2014) Hormonal control of cell division and elongation along differentiation trajectories in roots. J Exp Bot **65**: 2633–2643

Toledo-Ortiz G, Huq E, Quail PH (2003) The Arabidopsis basic/helix-loop-helix transcription factor family. Plant Cell **15**: 1749

Vanstraelen M, Benková E (2012) Hormonal interactions in the regulation of plant development. Annu Rev Cell Dev Biol **28**: 463–487

Werner T, Motyka V, Laucou V, Smets R, Van Onckelen H, Schmülling T (2003) Cytokinin-deficient transgenic Arabidopsis plants show multiple developmental alterations indicating opposite functions of cytokinins in the regulation of shoot and root meristem activity. Plant Cell **15**: 2532–2550

Wybouw B, De Rybel B (2019) Cytokinin - a developing story. Trends Plant Sci **24**: 177–185

Zhang WJ, Swarup R, Bennett M, Schaller GE, Kieber JJ (2013) Cytokinin induces cell division in the quiescent center of the Arabidopsis root apical meristem. Curr Biol **23**: 1979–1989

Zhao Z, Andersen SU, Ljung K, Dolezal K, Miotk A, Schultheiss SJ, Lohmann JU (2010) Hormonal control of the shoot stem-cell niche. Nature **465**: 1089–1092

Zubo YO, Blakley IC, Yamburenko MV, Worthen JM, Street IH, Franco-Zorrilla JM, Zhang W, Hill K, Raines T, Solano R, et al. (2017) Cytokinin induces genome-wide binding of the type-B response regulator ARR10 to regulate growth and development in *Arabidopsis*. Proc Natl Acad Sci USA **114**: E5995